Research Article | Vol. 25, No. 25 | 11 Dec 2017 | OPTICS EXPRESS 31552
Optics EXPRESS

Sensitive detection of voltage transients using differential intensity surface plasmon resonance system

SIDAHMED A. ABAYZEED,[1,*] RICHARD J. SMITH,[1] KEVIN F. WEBB,[1] AND MICHAEL G. SOMEKH,[2] AND CHUNG W. SEE [1]

[1]*Optics and Photonics Research Group, University of Nottingham, Nottingham, NG7 2RD, UK*
[2]*Electronic and Information Engineering, The Hong Kong Polytechnic University, Hung Hom, Kowloon, Hong Kong, China*
[*]*sidahmed.abayzeed@nottingham.ac.uk*

Abstract: This paper describes theoretical and experimental study of the fundamentals of using surface plasmon resonance (SPR) for label-free detection of voltage. Plasmonic voltage sensing relies on the capacitive properties of metal-electrolyte interface that are governed by electrostatic interactions between charge carriers in both phases. Externally-applied voltage leads to changes in the free electron density in the surface of the metal, shifting the SPR position. The study shows the effects of the applied voltage on the shape of the SPR curve. It also provides a comparison between the theoretical and experimental response to the applied voltage. The response is presented in a universal term that can be used to assess the voltage sensitivity of different SPR instruments. Finally, it demonstrates the capacity of the SPR system in resolving dynamic voltage signals; a detection limit of 10mV with a temporal resolution of 5ms is achievable. These findings pave the way for the use of SPR systems in the detection of electrical activity of biological cells.

OCIS codes: (240.6680) Surface plasmons; (280.4788) Optical sensing and sensors.

References and links

1. H. Raether, *Surface Plasmons on Smooth and Rough Surfaces and on Gratings* (Springer, 1986).
2. S. A. Abayzeed, R. J. Smith, K. F. Webb, M. G. Somekh, and C. W. See, "Responsivity of the differential-intensity surface plasmon resonance instrument," Sens. Actuators, B **235**, 627–635 (2016).
3. H.-M. Tan, S. Pechprasarn, J. Zhang, M. C. Pitter, and M. G. Somekh, "High resolution quantitative angle-scanning widefield surface plasmon microscopy," Sci. Rep. **6**, 20195 (2016).
4. A. Kabashin and P. Nikitin, "Surface plasmon resonance interferometer for bio-and chemical-sensors," Opt. Commun. **150**, 5–8 (1998).
5. A. Kabashin and P. I. Nikitin, "Interferometer based on a surface-plasmon resonance for sensor applications," Quant. Electron. **27**, 653–654 (1997).
6. G. Stabler, M. Somekh, and C. See, "High-resolution wide-field surface plasmon microscopy," J. Microsc. **214**, 328–333 (2004).
7. O. Bolduc, L. Live, and J.-F. Masson, "High-resolution surface plasmon resonance sensors based on a dove prism," Talanta **77**, 1680–1687 (2009).
8. J. Homola, "Surface plasmon resonance sensors for detection of chemical and biological species," Chem. Rev. **108**, 462–493 (2008).
9. R. J. Green, R. A. Frazier, K. M. Shakesheff, M. C. Davies, C. J. Roberts, and S. J. Tendler, "Surface plasmon resonance analysis of dynamic biological interactions with biomaterials," Biomaterials **21**, 1823–1835 (2000).
10. R. L. Rich and D. G. Myszka, "Advances in surface plasmon resonance biosensor analysis," Curr Opin Biotechnol. **11**, 54–61 (2000).
11. D. Kröger, F. Hucho, and H. Vogel, "Ligand binding to nicotinic acetylcholine receptor investigated by surface plasmon resonance," Anal. Chem. **71**, 3157–3165 (1999).
12. K. Kato, T. Ishimuro, Y. Arima, I. Hirata, and H. Iwata, "High-throughput immunophenotyping by surface plasmon resonance imaging," Anal. Chem. **79**, 8616–8623 (2007).

#301102 https://doi.org/10.1364/OE.25.031552
Journal © 2017 Received 21 Jul 2017; revised 7 Sep 2017; accepted 7 Sep 2017; published 4 Dec 2017

Optics EXPRESS

13. M. A. Jamil, F. Sefat, S. Khaghani, S. Lobo, F. A. Javid, M. Youseffi, S. Britland, S. Liu, C. See, M. Somekh, and M. Denyer, "Cell imaging with the widefield surface plasmon microscope," in "4th Kuala Lumpur International Conference on Biomedical Engineering 2008," (Springer, 2008), pp. 528–531.
14. A. M. Lopatynskyi, O. G. Lopatynska, M. D. Guiver, L. V. Poperenko, and V. I. Chegel, "Factor of interfacial potential for the surface plasmon-polariton resonance sensor response," Semicond. Phys. Quantum Electron. Optoelectron **11**, 329–336 (2008).
15. V. Lioubimov, A. Kolomenskii, A. Mershin, D. Nanopoulos, and H. Schuessler, "Effect of varying electric potential on surface-plasmon resonance sensing," Appl. Opt. **43**, 3426–3432 (2004).
16. K. Foley, X. Shan, and N. J. Tao, "Surface impedance imaging technique," Anal. Chem. **80**, 5146–5151 (2008).
17. Y. Huang, M. Pitter, and M. Somekh, "Morphology-dependent voltage sensitivity of a gold nanostructure," Langmuir **27**, 13950–13961 (2011).
18. Y. Huang, M. Pitter, and M. Somekh, "Time-dependent scattering of ultrathin gold film under potential perturbation," ACS Appl. Mater. Interfaces **4**, 3829–3836 (2012).
19. X. Shan, U. Patel, S. Wang, R. Iglesias, and N. Tao, "Imaging local electrochemical current via surface plasmon resonance," Science **327**, 1363–1366 (2010).
20. X. Shan, S. Wang, W. Wang, and N. Tao, "Plasmonic-based imaging of local square wave voltammetry," Anal. Chem. **83**, 7394–7399 (2011).
21. A. Dahlin, B. Dielacher, P. Rajendran, K. Sugihara, T. Sannomiya, M. Zenobi-Wong, and J. Vörös, "Electrochemical plasmonic sensors," Anal. Bioanal. Chem. **402**, 1773–1784 (2012).
22. F. Abeles, T. Lopez-Rios, and A. Tadjeddine, "Investigation of the metal-electrolyte interface using surface plasma waves with ellipsometric detection," Solid State Commun. **16**, 843 – 847 (1975).
23. R. Katz, D. Kolb, and J. Sass, "Electron density effects in surface plasmon excitation on silver and gold electrodes," Surf. Sci. **69**, 359 – 364 (1977).
24. J. McIntyre, "Electrochemical modulation spectroscopy," Surf. Sci. **37**, 658 – 682 (1973).
25. A. J. Bard and L. R. Faulkner, *Electrochemical Methods: Fundamentals and Applications* (Wiley New York, 2001).
26. B. Conway, *Electrochemical supercapacitors: scientific fundamentals and technological applications* (Springer Science & Business Media, 2013).
27. A. Katz, *Physiology of the Heart* (Lippincott Williams & Wilkins, 2010).
28. L. Loew, "Design and use of organic voltage sensitive dyes," in "Membrane potential imaging in the nervous system," (Springer, 2011), pp. 13–23.
29. T. H. Grandy, S. A. Greenfield, and I. M. Devonshire, "An evaluation of in vivo voltage-sensitive dyes: pharmacological side effects and signal-to-noise ratios after effective removal of brain-pulsation artifacts," J. Neurophysiol. **108**, 2931–2945 (2012).
30. S. Ae Kim, K. Min Byun, J. Lee, J. Hoon Kim, D. Albert Kim, H. Baac, M. Shuler, and S. June Kim, "Optical measurement of neural activity using surface plasmon resonance," Opt. Lett. **33**, 914–916 (2008).
31. S. Kim, S. Kim, H. Moon, and S. Jun, "In vivo optical neural recording using fiber-based surface plasmon resonance," Opt. Lett. **37**, 614–616 (2012).
32. J. E. Garland, K. A. Assiongbon, C. M. Pettit, and D. Roy, "Surface plasmon resonance transients at an electrochemical interface: time resolved measurements using a bicell photodiode," Anal. Chim. Acta **475**, 47–58 (2003).
33. Y. Huang, M. Pitter, M. Somekh, W. Zhang, W. Xie, H. Zhang, H. Wang, and S. Fang, "Plasmonic response of gold film to potential perturbation", Sci. China. Phys. Mech. Astron.**56**, 1495–1503 (2013).
34. R. Azzam and N. Bashara, *Ellipsometry and polarized light* (Elsevier science, 1987).
35. J. Zhang, T. Atay, and A. Nurmikko, "Optical detection of brain cell activity using plasmonic gold nanoparticles", Nano Lett. **9**, 519–524 (2009).
36. J. W. Schultze and G. Staikov, *Electrochemistry in Molecular and Microscopic Dimensions: Proceedings of the 53rd Annual Meeting of the International Society of Electrochemistry: Jointly Organized with the GDCh-Fachgruppe Angewandte Electrochemie, Düsseldorf, Germany, 15-20 September 2002*, vol. 48 (Elsevier, 2003).
37. A. D. Rakić, A. B. Djurišić, J. M. Elazar, and M. L. Majewski, "Optical properties of metallic films for vertical-cavity optoelectronic devices," Appl. Opt. **37**, 5271–5283 (1998).
38. P. B. Johnson and R. W. Christy, "Optical constants of the noble metals," Phys. Rev. B **6**, 4370–4379 (1972).
39. A. N. Bashkatov and E. Genina, "Water refractive index in dependence on temperature and wavelength: a simple approximation," Proc. SPIE **5068**, 393–395 (2003).
40. P. Schiebener, J. Straub, J. L. Sengers, and J. Gallagher, "Refractive index of water and steam as function of wavelength, temperature and density," J. Phys. Chem. Ref. Data **19**, 677–717 (1990).
41. M. H. George and R. Q. Marvin, "Optical constants of water in the 200-nm to 200-μm wavelength region," Appl. Opt. **12**, 555–563 (1973).
42. N. Tao, S. Boussaad, R. Huang, W.L.and Arechabaleta, and J. DÁgnese, "High resolution surface plasmon resonance spectroscopy," Rev. Sci. Instrum.**70**, 4656–4660 (1999).
43. Z. Kerner and T. Pajkossy, "On the origin of capacitance dispersion of rough electrodes," Electrochim. Acta **46**, 207–211 (2000).
44. W. Wang, K. Foley, X. Shan, S. Wang, S. Eaton, V. J. Nagaraj, P. Wiktor, U. Patel, and N. Tao, "Single cells and intracellular processes studied by a plasmonic-based electrochemical impedance microscopy," Nat. Chem. **3**, 249–255 (2011).

Optics EXPRESS

45. T. Pajkossy, "Impedance spectroscopy at interfaces of metals and aqueous solutions : surface roughness, CPE and related issues," Solid State Ion. **176**, 1997–2003 (2005).
46. C. Celedón, M. Flores, P. Häberle, and J. Valdés, "Surface roughness of thin gold films and its effects on the proton energy loss straggling," Braz. J. Phys. **36**, 956–959 (2006).
47. L. Daikhin, A. Kornyshev, and M. Urbakh, "Double layer capacitance on a rough metal surface: surface roughness measured by "Debye ruler"" electrochim. acta **42**, 2853–2860 (1997).
48. L. Daikhin, A. Kornyshev, and M. Urbakh, "Double-layer capacitance on a rough metal surface," Phys. Rev. E **53**, 6192 (1996).
49. J. Macdonald and M. Brachman, "The charging and discharging of nonlinear capacitors," Proceedings of the IRE **43**, 71–78 (1955).
50. K. Chu and M. Bazant, "Nonlinear electrochemical relaxation around conductors," Phys. Rev. E **74**, 011501 (2006).

1. Introduction

Surface plasmons (SPs) are light-excitable surface waves that are described as longitudinal oscillations of free electrons at the metal-dielectric interface. They oscillate with a spatial frequency greater than that of light in air. Using optical configurations [1] where the spatial frequency of light is increased, SPs are excited at the metal-dielectric interface. For instance, Kretschmann-Raether configuration is one of the commonly used experimental setups, in which a monochromatic p-polarised light is coupled through a prism [2]. Alternatively, an oil immersion high numerical aperture objective lens [3] is used. In both cases, surface plasmon resonance is achieved at specific angle of incidence. The excitation of SPs results in a drop of the intensity of the reflected light [2] and a sharp phase transition [4, 5] at the resonance angle [6] or wavelength [7]. This resonance is sensitive to the properties of the dielectric layer adjacent to the metal as well as the metal surface. This feature has been widely used to develop chemical and bio-sensors [8–10].

Surface plasmon resonance (SPR) systems are applied to sensing and imaging of interfacial processes. As they are sensitive to the optical properties of the dielectric medium, they have gained a great deal of interest in bio-medical research being used to probe molecular interactions within the evanescent field at the metal-dielectric interface [11], cell sensing [12] or imaging the cell membrane [13]. In addition to SPs sensitivity to the properties of the dielectric layer, they are also sensitive to the properties of the supporting metallic layer. As illustrated in Fig. 1, when external voltage is applied between the metal thin film and an electrolyte solution, an interfacial capacitance is charged. This effect alters the surface charge density, leads to changes in the optical properties of the metal and shifts the resonance position [14, 15]. This additional feature provides a different use of SPR systems for voltage sensing [14–18] opening new avenues in electrochemical applications [19–21].

Evidence of the voltage effect on the optical properties of the metal-electrolyte interface is not recent; for instance, the concept of voltage detection using SPR was demonstrated in a number of articles as early as 1970s [22, 23]. The effect has been attributed to the modification of the charge density in the metal surface by charging and discharging the double layer capacitor [24]; an interfacial nano-scale capacitor that is formed at the metal-electrolyte interface [25]. In other words, charge carriers in the electrolyte laminae adjacent to the metal are mirrored by the excess or deficiency of free electrons in the metal side. As shown in Fig. 1, the accumulated charge is confined within the Thomas-Fermi screening length of the metal due to penetration depth of the low-frequency electric field being limited to few angstroms (i.e. screened by the free electrons) [26]. Changes in the electron density modifies the optical properties of the metal layer and subsequently the spatial frequency of surface plasmons. The voltage sensing mechanism is described in more detail in Sec.3.1.

Voltage sensing is of a particular importance in biological applications. For instance, the depolarisation of cell membrane of the electrogenic cells is known to coordinate a number of vital physiological processes: the contractility of cardiomyocytes, for example [27]. The state

Optics EXPRESS

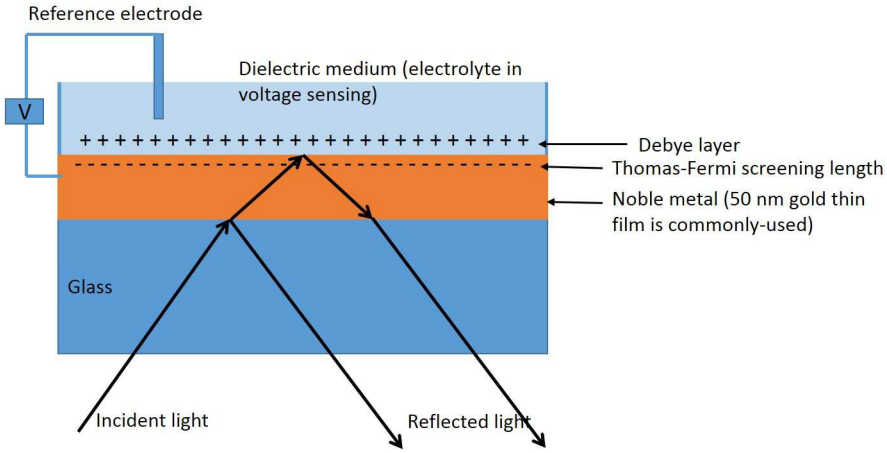

Fig. 1. The concept of voltage sensing using surface plasmon resonance sensors. Surface plasmons are sensitive to changes in charge density at the gold-electrolyte interface.

of the art measurement techniques include the use of voltage-sensitive dyes; membrane-bound molecules whose fluorescence intensity is sensitive to perturbations of electrical energy in their proximity [28]. Despite their ability to reveal subcellular information, fluorescence measurements are affected by photobleaching, which limits the timescale of experiments and fluorescent labels can also be toxic to cells [29]. Therefore, SPR sensors are being investigated as a potential label-free, non-invasive method for the detection of the bio-electrical signals [30, 31]. The sensitivity of SPR to surface charge density provides a direct method of detecting voltage signals. This study is directed at investigating the fundamentals of using SPR voltage sensors for biological applications. In particular, the study addresses four important aspects: voltage effects on the SPR curve; characterisation of the response of SPR systems to externally applied voltage; comparison between theoretical and experimental approaches; and detection of time-resolved voltage signals. The significance of these four points will be discussed briefly in Sec.2.

2. Voltage sensing using SPR systems

This section presents a brief review and discussions of the previous work in voltage sensing using surface plasmon resonance systems. We highlight aspects that are important for understanding and characterising the performance of SPR systems in voltage sensing applications.

2.1. Voltage effects on the SPR curve

In order to design SPR systems with optical configurations that are suitable to voltage sensing, voltage effects on SPR curve were discussed in previous studies. For instance, Garland et al [32] addressed changes in the shape of SPR curve during voltage perturbations. The study considered a voltage range that is wider than the double layer capacitance charging window that can induce electrochemical reactions. Changes to the shape of SPR curve under low voltage excitation are not explained. Since this article is focused on sensing small voltage within the double layer capacitance charging window, the effect on the SPR curve is studied as presented in Sec.4.1. Understanding this effect is necessary to the design of highly sensitive SPR systems for voltage sensing applications.

Optics EXPRESS

2.2. Comparison between theoretical and experimental approaches

Theoretical analysis provides a relatively simple way to understand the response of SPR under voltage perturbations that allows investigation of different experimental conditions. Theoretical studies of voltage sensing using SPR combines both optical and electrochemical models. Optical models investigate light propagation and reflection from the multi-layer SPR sensing structure while electrochemical models describe the behavior of the interfacial capacitance. SPR sensing structure is studied using the well-known matrix transfer method and Fresnel equations [34]. From this model, SPs excitation is studied under different experimental conditions. In order to study the voltage effect on the properties of the sensing structure, two approaches for modeling the interfacial capacitance are used. The first approach models the capacitive properties of the interface with a linear parallel-plate capacitor [16]. This approach offers simplicity over the well-known properties of Stern-Gouy-Chapman capacitance. The second approach uses the non-linear capacitance model of Stern - Gouy Chapman [14], in which the interfacial capacitance is estimated more accurately considering the electrolyte concentration and the applied voltage. Although, theoretical models were presented in a number of previous studies [14, 15], a rigorous comparison between theoretical and experimental voltage sensing using SPR has not been provided. In this study, we present comparison between predicted and experimental SPR response to voltage (see Sec.4.2). Furthermore, we comment on the origin of the nonlinear response of the system and its implications on the sensitivity of the system.

2.3. Characterisation of the response of SPR systems to externally applied voltage

In order to study the response of SPR sensors to voltage in the context of biological applications, two factors need to be addressed. First, the response of the SPR systems has to be characterised for an electrolyte solution that simulates the ionic properties of the extracellular solution since the properties of the gold-electrolyte interface is an important factor in voltage sensing. Second, this response needs to be generalised so the obtained results can be applied to different types of SPR instruments, regardless of their detection scheme.

Voltage detection with SPR has been investigated using different types of electrolyte solutions. For instance, Lioubimov et al [15] reported different amplitude responses (i.e. resonance shift) of the SPR when pure water, 5mM NaCl, 5mM KOH and propionic acid are used as electrolytes. Nonetheless, the obtained results cannot be used to draw a conclusion on SPR response to voltage for biological applications. This factor was addressed previously in [33]. In this study, we present a universal measure for the voltage responsivity of SPR systems for biomedical applications. Since SPR systems are characterised by their response to refractive index change, we measured the voltage-equivalent refractive index change experimentally compared to the theoretical prediction, as presented in Sec.4.3. The voltage-equivalent refractive index change can be used to quantify the performance of SPR systems for their response to voltage, regardless of the used optical system configuration.

2.4. Detection of time-resolved voltage signals

Label-free detection of time-resolved bioelectrical signals is investigated as a new tool for biomedical research. The advantage of this approach is its non-invasiveness, unlike the currently-used micro-electrode methods, and moreover it overcomes phototoxicity related to the use of fluorescent dyes. It brings the potential of studying biological systems at their cellular scale, in their natural state and over long periods of time. For instance electrical signals, typically in the millisecond range, are used by neuronal cells to coordinate the function of the nervous system. Label-free detection of these signals open new horizons in understanding the function of the brain and the nervous system. In this study, we investigate the capacity of SPR systems, as a label-free technique, as candidates for the detection of these voltage signals.

Optics EXPRESS

The response of the SPR to dynamic voltage excitations has not been considered in detail in the present literature. For instance, in [15], Lioubimov et al measured the response of for a sweep over a low frequency range (2mHz - 0.2Hz). The results obtained showed a drop in the response of the sensor as the frequency of voltage signal increases. Similar drop is observed by Huang et al [18] when studying the response of plasmonic nanostructures to dynamic voltage signals. The study discussed the contribution of the frequency dispersion of the double layer capacitor to the observed decrease in the response. In this study, we demonstrated detection of dynamic voltage signals with a temporal resolution of 5 ms and a detection limit of 10mV; the smallest reported detection limit using SPR systems to the best of our knowledge. Furthermore, we discussed the factors of the drop in the response of SPR systems under excitation with dynamic time-resolved signals.

3. Methods

3.1. Modeling

This section describes the procedure for modeling the response of SPR systems to an externally applied voltage. As mentioned in the introduction, surface plasmon resonance is sensitive to the free electrons density in the metallic layer. When voltage is applied to the gold-electrolyte interface, change in charge density at the interface results in the modification of the dielectric constant of the surface layer of the metal and subsequently shifts the resonance position.

In order to simulate the effect of the interfacial potential on surface plasmon resonance, we followed a protocol that calculates the interfacial capacitance under the influence of the applied voltage and the concentration of the electrolyte. The capacitive properties of the interface have been simulated using the well-known Gouy-Chapman-Stern model which takes into account, in addition to the applied voltage, the factors of the electrolyte such as valence, ion density and permittivity [25]. This model is combined to a one dimensional multilayer system that models the optical properties of the SPR sensing structure, as shown in Fig. 2. As demonstrated in Fig. 3, this model can also be used to simulate the potential profile at the metal-electrolyte interface. The modeling procedure is performed under two assumptions:

(i) The effect of the applied voltage on the dielectric properties of the electrolyte is negligible. As shown in Fig. 3, the effective voltage sensing depth in the electrolyte (Debye layer ~ 1 nm) is very small compared to the evanescent field depth (in the order of 100 nm).

(ii) The metal thin film is simulated with two layers: Thomas-Fermi length and the bulk gold. The model assumes an abrupt interface between the two layers. This is a simplification to the decay of the low frequency electric field from the metal surface towards the bulk with a depth equivalent to Thomas-Fermi length.

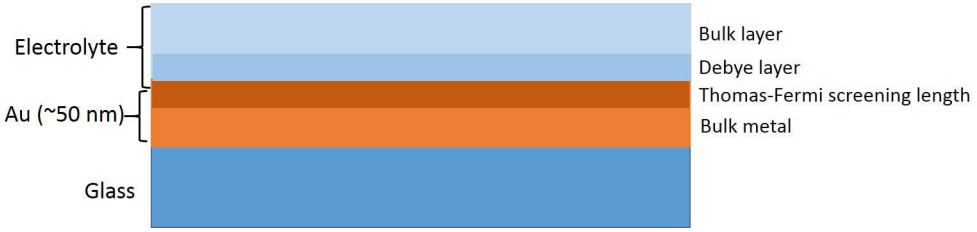

Fig. 2. One dimensional model of the sensing structure showing the glass substrate coated with 50 nm of gold while the electrolyte is placed on the top of the gold surface. Debye and Thomas Fermi layers are highlighted in electrolyte and gold respectively.

Optics EXPRESS

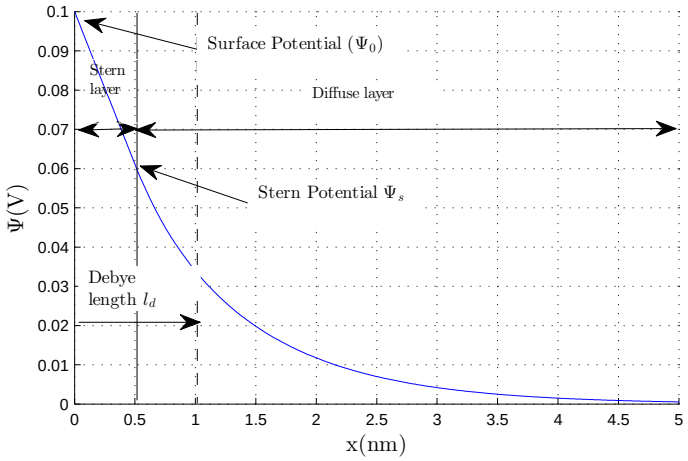

Fig. 3. The graph shows the key regions in a metal-electrolyte interface that are formed due to the extended electrostatic interactions between charge carriers in the metal and the electrolyte. The Stern layer is formed by electrostatic interaction similar to parallel-plate capacitor while diffuse layer is formed due to competitive effect of the thermal energy and electrostatic potential. The Debye layer is the depth at which the potential drops to 1/e of its initial value. The profile is simulated for a 0.15M NaCl.

We implemented the following steps for voltage series between (-200mV and +200 mV) to produce resonance curves for each voltage which were used to investigate the effect of the voltage on the resonance curve.

(a) The value of the electrical double layer capacitance of the interface was calculated taking into consideration the ion density (n_0) in the electrolyte and the applied voltage (ψ_0). The electrical double layer capacitance is a nano-scale capacitor that is formed at the metal electrolyte interface due to the electrostatic interactions between the ions in the electrolyte (in the Debye layer) and the free electrons in the metal (in the Thomas-Fermi layer). The phenomena is well described in standard physical chemistry and electrochemistry texts [25]. It is formed of two capacitances in series as presented in Eq. (1). The first is confined to the metal surface and behaves like a parallel-plate capacitor with a separating layer characterized by the dielectric properties of the solvent and has a thickness in the order of the size of its molecules. The second is a result of the extension of the electrostatic potential to a few nanometers into the electrolyte and its penetration depth depends on the charge density. Therefore, it depends both on the applied potential (ψ_0) and the concentration of the electrolyte (See Eq. (1) [25]).

$$\frac{1}{C} = \frac{x_s}{\epsilon_0 \epsilon} + \frac{1}{\sqrt{\frac{2\,\epsilon_0\,\epsilon\,n_0\,z^2\,e^2}{kT}}\cosh\left(\frac{ze\psi_s}{2kT}\right)} \tag{1}$$

where the size of the solvent molecule (x_s) is 0.5 nm [15] (the water in this case), the static permittivity of water(ϵ) is 80 at 20°C [35], the valence of the ion (z) is 1 for NaCl, the elementary charge (e) is 1.602×10^{-19}C, thermal energy (kT) is 4.1164×10^{21} J and ψ_s is the Stern potential, which was found by solving Eq. (2) [25] with the conditions $\psi = \psi_s$ at $x = x_s$.

Optics EXPRESS

$$\psi(x) = \psi_0 - x\sqrt{\frac{8kTn_0}{\epsilon_0\epsilon}}\sinh\left(\frac{ze\psi_s}{2kT}\right) \tag{2}$$

(b) Applying the McItyre model (Eq. (3)), the change in the density of free electrons (ΔN) was calculated using the capacitance (C) obtained in the previous step, the applied potential (ψ_0) and Thomas-Fermi length ($d_{TF} = 0.5A°$) [36]. Then, the obtained value is used to calculate the plasma frequency (Eq. (4)).

$$\Delta N = \frac{C\psi_0}{-ed_{TF}} \tag{3}$$

$$\omega_p = \sqrt{\frac{(N + \Delta N)e^2}{m\epsilon_0}} \tag{4}$$

where ω_p is plasma frequency, the free-space permittivity (ϵ_0) is 8.85×10^{-12} F/m, the mass of the electron (m) is 9.12×10^{-31} kg and e is elementary charge.

(c) The dielectric constant ($\epsilon(\omega)$) of Thomas-Fermi length was calculated from Drude model (Eq. (5)) for each applied potential.

$$\epsilon(\omega) = 1 - f_0\frac{{\omega_p}^2}{\omega(\omega + i\gamma)} \tag{5}$$

where γ is the damping constant, ω_p is the plasma frequency and f_0 is the oscillator strength of the intraband transitions. Values for these parameters were obtained from [37].

(d) SPR curves were produced for the sensing structure described in Fig. 2 that consist of glass ($n_0 = 1.5151$), bulk gold($n_2 = 0.18344 + 3.4332i$ [38]), Thomas-Fermi length (with voltage dependent dielectric constant and thickness of 0.5 A° [36]) and a semi-infinite layer of electrolyte solution ($n_3 = 1.33339$ at $20°C$ calculated with compensation for temperature and wavelength from [39–41]). All refractive indices were obtained for a wavelength of 633nm. To produce SPR curves, the transfer matrix method (TMM) described in [14, 34] was used to calculate the reflected coefficient of p-polarised light for a range of angles of incidence.

(e) Changes in the resonance position associated with the applied voltage ($\Delta\theta_0$) were calculated by tracking the change in the location of the minimum reflectivity of the SPR curve.

(f) The sensing structure described in Fig. 2 was used to find the relation between the change in the refractive index (Δn) and the change in the resonance angle ($\Delta\theta_0$) for mapping the effect of the voltage to its equivalent refractive index. For this purpose, refractive index of the electrolyte was stepped while no voltage is applied to the interface.

3.2. Experiments

The experimental validation of SPR response to voltage was performed by combining a three electrode electrochemical cell (from Reichert Technologies Life Sciences) with a differential intensity surface plasmon resonance system [2, 42]. In this setup, a 50nm gold thin film, deposited on a Bk-7 glass slide by sputtering, was used as a working electrode, Ag/AgCl in 3M NaCl was used as a reference electrode and a platinum electrode was a used as an auxiliary electrode.

Optics EXPRESS

This electrochemical cell was connected to a potentiostat (VersaStat 3 from Princeton Applied Research) to apply a voltage between the metal surface and the electrolyte (i.e.the working electrode and the reference electrode in Fig. 4). Voltage sensing experiments were performed using 0.15M NaCl as an electrolyte. Different voltage modulation waveforms in the range of ($\pm 200mV$) were applied versus the reference electrode while SPR response was recorded simultaneously using the optical system. It is noted that the potential of zero charge (PZC), for the gold thin film in 0.15M NaCl, was -10 mV with respect to the reference electrode when measured by finding the minimum of the differential capacitance curve.

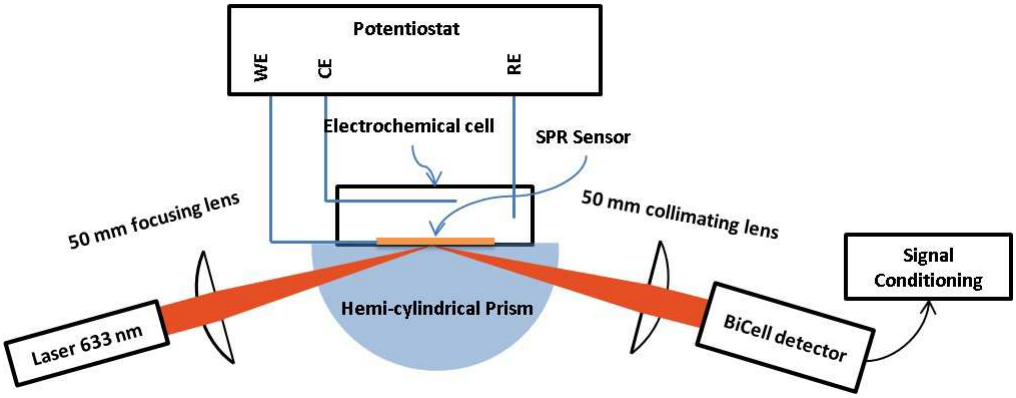

Fig. 4. Electrochemical Surface Plasmon Resonance System: a prism based Kretchmann-Raether configuration, that is used to excite surface plasmons at the metal-electrolyte interface. A three electrode, electrochemical cell is mounted on the prism, which is used to modulate the potential at the metal-electrolyte interface.

The DI-SPR sensing system used a prism-based Kretschmann-Raether configuration (Fig. 4), in which a beam of p-polarized light ($\lambda = 633nm$) is weakly focused on the metal surface and the average angle of incidence is the resonance angle so that surface plasmons are excited at the interface between the metal and the electrolyte - 0.15M NaCl. The reflected light is collimated by a cylindrical lens (50 mm) before detected with a bicell photodiode. The output of the bicell detector is used to calculate the differential response. Assuming the outputs of the two halves of the detector be A & B respectively, the differential response is defined as (A-B)/(A+B), as explained in [42]. The process is performed in real time, using a home-made electronic circuit to perform the difference and the sum. A 16 bit data acquisition device is used for analog to digital conversion. The bicell detector is balanced, initially, to operate at the point of maximum sensitivity [2]. As explained in previous publications [2, 42], the output of the processed bicell detector signal (A-B)/(A+B) is directly proportional to the change in the resonance angle. The analytical expression described in the previous publication [2] was used to retrieve the resonance angle shift from the output of the bicell photodetection. The resonance angle shift was mapped to the equivalent refractive index change to calculate the experimental voltage equivalent refractive index change.

4. Results and discussions

In this section, we present and discuss the factors that affect voltage detection using differential intensity surface plasmon resonance (DI-SPR) system. First, we present the effects of the applied voltage on the SPR curve using theoretical modeling of voltage sensing using SPR sensors. Second, we present a comparison between theoretical and experimental response to applied voltage. Also, the response is presented in terms of the equivalent refractive index change;

a generally applicable parameter that can be used to assess the voltage sensitivity of a range of SPR systems. Finally, we show the detection of time-resolved voltage transients over the millisecond range with a detection limit of 10mV.

4.1. Voltage effects on the SPR curve

To investigate the sensitivity of SPR systems in the detection of voltage perturbations, we start with characterising the effect of the externally applied voltage on the SPR curve. Theoretical approaches, described in Sec.3.1, were used to simulate SPR curves for a series of voltages in the range of (-0.2 V to 0.2 V), as presented in Fig. 5. As observed from this figure, increasing the voltage increases the resonance angle and vice versa. Furthermore, the effect of the voltage on the resonance angle is compared to its effect on the the full-width half-maximum of the curve and the minimum of the reflectivity (Fig. 6). This comparison is important to see which effect is dominant and therefore worth measuring to obtain a better signal-to-noise ratio. As confirmed by Fig. 6 that the shift in resonance position is significant compared to the change in the shape of the SPR curve and the minimum of the curve.

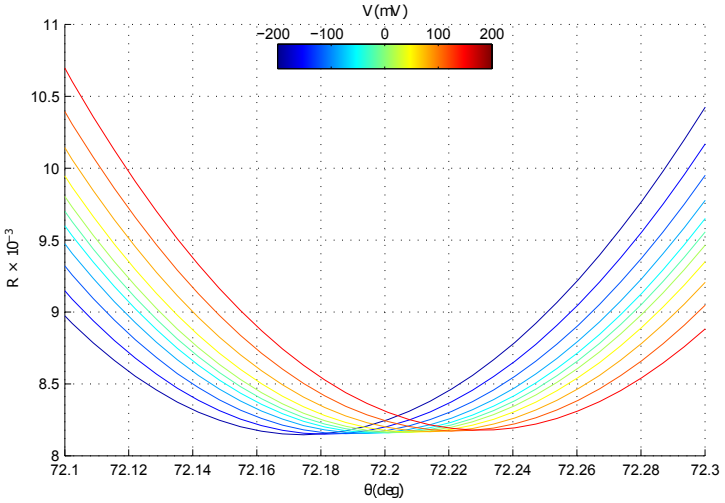

Fig. 5. The effect of the applied voltage on the SPR curve. Theoretical SPR curves were generated for a sensing structure formed of BK-7 glass coated with 50 nm of gold. The wavelength of the incident light is 632.8nm. Voltage series were simulated for 0.9% sodium chloride as an electrolyte solution.

The information about the effects on the curve complements the study performed by Garland et al [32] which reports on voltage effects on SPR curve . However, it is noted that our results are only valid for the double layer voltage window ($\pm 200mV$). Further increase of the applied voltage could trigger electrochemical processes on the gold surface which change the shape of the SPR curve significantly [32]. Knowledge on the effect of the voltage on the shape of the SPR curve is important for the choice of the SPR system. In this study, the DI-SPR technique was used since it provides a sensitive detection of resonance angle shift in the range of 10^{-6} – 10^{-5} deg (i.e.10^{-8} – 10^{-7}RIU) [42].

4.2. SPR response to the applied voltage

To study how the resonance angle changes with the externally-applied voltage, the waveform in Fig. 7(a) has been applied to the gold-electrolyte interface using the three electrode system

Optics EXPRESS

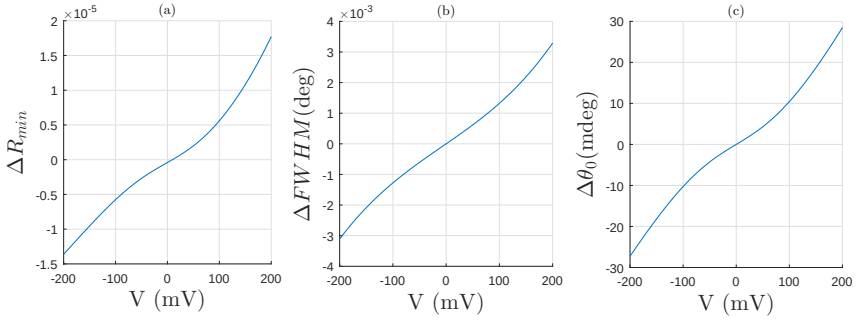

Fig. 6. The effects of the applied voltage on the properties of the SPR simulated using the procedure described in Sec.3.1. Change to the minimum reflectivity is shown in (a) while changes to the full-width half-maximum (FWHM) and the resonance angle are presented in (b) and (c) respectively.

described in Sec.3.2. The response of the SPR to the applied waveform is measured by using the DI-SPR setup described in Sec.3.2 as presented in Fig. 7(b). From this graph, it is observed that for each of the applied voltages, the system does not respond instantaneously as it is governed by charging the double-layer capacitor which features a remarkably high capacitance in the order of $1F/m^2$ [25]. Since the system features a time-varying response, the ratio (A-B)/(A+B) is used, after reaching equilibrium of each voltage step, to calculate the equivalent angular shift by using the protocol described previously [2]. Figure 8 presents the change in the resonance angle for each voltage step compared to the theoretical resonance angle shift obtained using the procedure in Sec. 3.1.

The system demonstrated a noticeable nonlinear response to the applied voltage regardless of its polarity confirming the behavior the nonlinear voltage dependent double-layer capacitance of the interface. Another observation is the asymmetry between the positive and the negative cycles of voltage. Positive voltage cycles, with respect to the potential of zero charge, show higher response, especially at higher potentials. A similar effect has been reported previously in voltage sensing using plasmonic structures [18]. Since the supporting electrolyte contains chloride ions, this observation could be attributed to the preferential interaction of halides with gold surfaces [43]. The specific adsorption of anions affects the shape of the differential capacitance curve (*vs* potential) for voltages higher than the potential of zero charge (PZC). The observed discrepancy between theoretical and experimental results is discussed in the next section.

4.3. Voltage-equivalent refractive index change

Generally, the sensitivity of SPR systems is characterized in terms of refractive index change. By mapping the obtained voltage response to its equivalent refractive index change, a universal term for voltage response or sensitivity is obtained. As shown in Fig. 9 the voltage equivalent refractive index change is calculated, as described in Sec.3.1, using both experimental and theoretical approaches. The graph presents a good agreement between the theoretical and the experimental response, compared to previous studies [15] in which theoretical and experimental results do not show such close correspondence. Such an agreement between theoretical and experimental response is reported for the first time, to the best of our knowledge, supporting the use of the proposed 1D model to estimate the response of SPR systems to externally applied voltage. The consequences of using the 1D model are discussed in the next paragraph.

As the use of surface plasmon resonance for voltage sensing for biological applications [44] is increasing, obtaining a generic term for estimating voltage sensitivity of SPR is valuable as it gives a universal means of comparison. It can be used when designing experiments or devel-

Optics EXPRESS

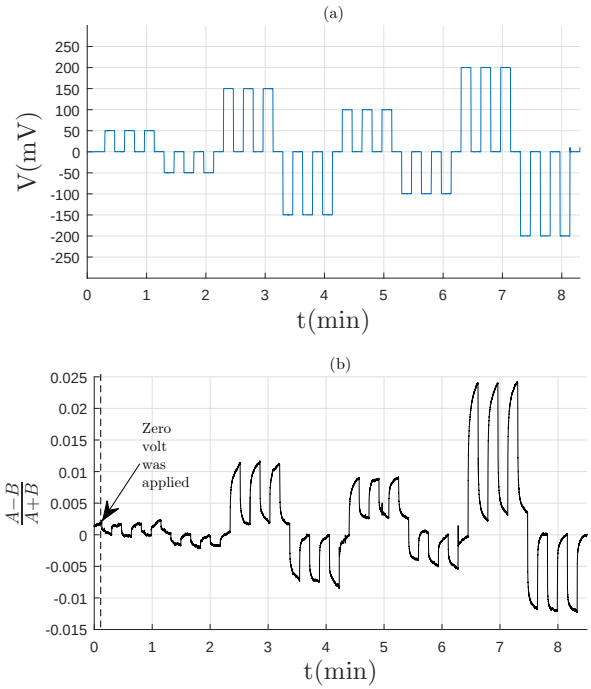

Fig. 7. (a) The input voltage waveform. Voltage is applied versus an Ag/AgCl reference electrode at a rate of 10V/s (b) The response of the DI-SPR system to the input waveform for 0.15M NaCl.

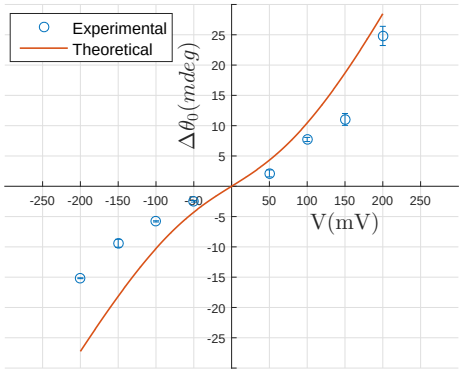

Fig. 8. Experimental resonance shifts ($\Delta\theta_0$) for a series of applied voltages compared to theoretical resonance angle shift.

oping sensitive instruments to probe biological processes. Although the experimental and theoretical results demonstrated a good agreement, there is still a discrepancy between them.The theoretical results are based on modeling a one dimensional metal-electrolyte structure assuming an ideal case of using flat monocrystalline gold surfaces. As discussed in Pajkossy [45], the non-ideal surface structure showed a different capacitive behavior. On the other hand, the experimental results were obtained using polycrystalline surfaces [14, 15, 46] with no further treatment. To model the voltage sensitivity of the polycrystalline surface, one needs to use a 2D

Optics EXPRESS

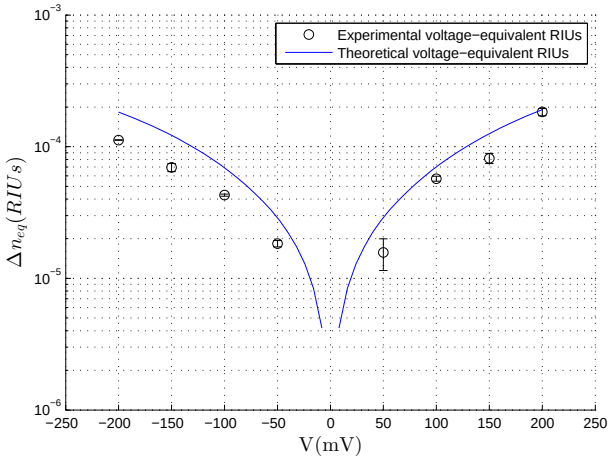

Fig. 9. Experimental voltage-equivalent refractive index units compared to theoretically calculated figures.

model to account for the effect of the roughness. The spatial profile of the capacitive properties of the interface has to be modeled with a lateral resolution that is sufficiently fine for the periodicity of the roughness. The contribution of the surface roughness and structure to the capacitive properties of the surface was discussed in literature [47,48]. Nevertheless, the model used in this study is a reasonable approximation that can be used to study SPR sensors for voltage sensing applications.

It should be noted that the sensitivity reported in this study is enhanced compared to the previous work [18]; a detection limit of 1 mV is achieved. The DI-SPR noise is calculated, for a time scale of 1 second, which is 5 $\times 10^{-5}$. Since the DI-SPR response is 5 $\times 10^{-3}$ for 100 mV, the detection limit is therefore expected to be 1mV. This maps to 3.7 $\times 10^{-7}$ RIUs for these experimental conditions. The enhancement of sensitivity is attributed to the removal of the correlated noise between the two units of the bicell detector by using differential detection and further improvement with normalisation to the total detected power. The correlated noise arises from the fluctuations of the laser power which dominates the time resolved measurements and deteriorate the sensitivity.

4.4. Time-resolved detection of interfacial potential

Examining the temporal resolution of SPR voltage sensors is crucial to detecting time-resolved biological processes, which occurs over a millisecond timescale (e.g. action potential generated by a neuron). In this section, a pulse train with 100 mV magnitude, 5 ms width and 1s separation was generated using the potentiostat as described in Sec.3.2 and applied to the gold-electrolyte interface. The response of the DI-SPR system to the applied pulse train is presented in Fig. 10. The applied voltage and current are shown in Figs. 10(a) and 10(b) respectively compared to the SPR response presented in Fig. 10(c). The voltage, the current and the SPR response are presented over a magnified scale in Figs. 10(d)-10(f) respectively. The response of the SPR sensor is directly related to the applied voltage waveform as it is expected from the direct relation of the resonance angle shift to surface charge density that is explained in Sec.3.1 in detail. The 5 millisecond pulses shows a lower response compared to the previous 10 second signals. As a consequence, the sensitivity drops from 1 mV to 10 mV as the response of the system drops by an order of magnitude.

The temporal resolution of the system is affected by the voltage dependence nature of the double layer capacitor which results in a non-linear system making the time constant a time-varying

Optics EXPRESS

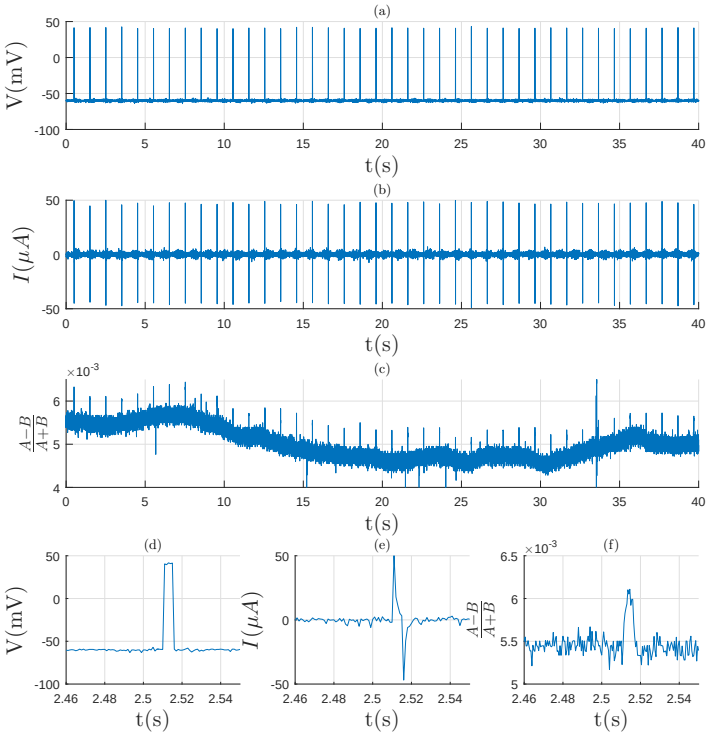

Fig. 10. The DI-SPR response to voltage pulses with a duration of 5ms. In (a) the applied 100mV voltage signals and corresponding charging and discharging currents are shown in (b). The simultaneous SPR response is presented in (c). (d-f) shows the a window of the three signals on a magnified scale.

quantity. In the following section, the response time is discussed in more detail considering the response of the system to 100 mV applied for 10 seconds as an example.

4.5. *Response time of the gold-electrolyte interface to applied voltage*

When voltage is applied to the electrode-electrolyte interface, surface charge density is altered charging the interfacial double-layer capacitor. The accumulation of charges in the Debye layer is not instantaneous, compared to the applied voltage. In order to quantify the dynamics of this process, the SPR response to a potential change from 0 to +100 mV is investigated. It can be seen from Fig. 11(a) that the response time of the sensor does not fit to a first order exponential function with time constant $\tau = RC$. It is rather approximated to fit a second order exponential function $y(t)$ below (goodness of fit: $R^2 = 0.993$ and root-mean-square error ($RMSE$) = 6.8×10^{-5}).

$$y(t) = a_1(1 - e^{-t/\tau_1}) + a_2(1 - e^{-t/\tau_2}) + c \tag{6}$$

where $\tau_1 = 37ms, \tau_2 = 1.35s$ are time constants and $a_1 = 2.4 \times 10^{-3}$ and $a_2 = 3 \times 10^{-3}$ are steady state amplitudes and c=0.0033.

The graph in Fig. 11(a) demonstrates the behavior of a non-linear system with a time-varying charging rate, which can be approximated by two processes with different dynamics: a fast

Optics EXPRESS

response with a time constant of 37 ms and a slow response with a time constant of 1.36s. The time constants and the occurrences of these processes can be visualized better by looking at the charging rate obtained by taking the derivative of Eq. (6):

$$y'(t) = \frac{a_1}{\tau_1} e^{-t/\tau_1} + \frac{a_2}{\tau_2} e^{-t/\tau_2} \tag{7}$$

With the same definitions of the coefficients of Eq. (6). Plotting the natural logarithm of $y'(t)$ versus time compared to the natural logarithm of the first and the second term shows the overall response compared to the fast and slow responses. The dynamics observed in Fig. 11(b) is consistent with the reported response of charging nonlinear capacitors [49]. As the diffuse layer capacitor is voltage dependent, the behaviour of the system follows nonlinear dynamics with a time constant that also depends on the applied voltage. The nonlinear capacitance is reported to extend the charging time resulting in the slow response [50]. However, in this discussion, the response is simplified by fitting to the second order function presented by Eq. (6). Therefore, the time-varying response is characterised by two time constants τ_1 and τ_2 which are dominant for the ranges $t \leq 0.2$ and $t > 0.2$ respectively.

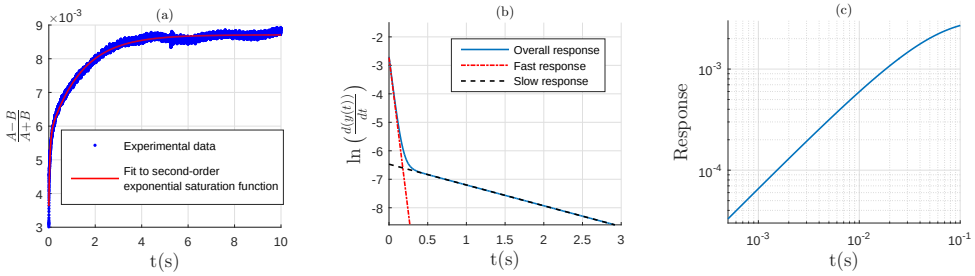

Fig. 11. (a) Dynamic response of the SPR system to the applied voltage (100mV) fitted to a second-order exponential saturation function. (b) A comparison between time constants and onset times of the fast and the slow responses of the system to the applied voltage. (c) Expected response of the system for pulses with duration less than $0.2s(5\tau$ of the fast response).

The first term of the fitted function in Eq. (6) can be used to predict the response of the SPR system to pulses with short duration ($\leq$ 0.2 or $5\tau_1$). The expected response of the system, for pulses less than 0.2s, is presented in Fig. 11(c). As can be found from this graph, the response drops to 3×10^{-4} for pulses with a duration of 5ms. This response drop agrees with the SPR response to 5ms pulses shown in Figs. 10(c) and 10(e). This analysis can be used to predict the time dependent response of the system to the action potential of neurons since the pulse last only for 2- 5 ms.

5. Conclusions

In this study, we present the fundamentals of using SPR systems for voltage sensing applied to biological research questions. First, the study investigated the effect of the externally applied voltage on the shape and the resonance position of the SPR curve. We found that for voltage in the range of $\pm 200mV$, the shift in the resonance position depends on the polarity of the applied voltage while the shape of the SPR curve is preserved under low voltage excitations. This finding guides the selection of optical configuration for voltage sensing. Second, a rigorous comparison between theoretical and experimental response of SPR to voltage is presented. The results are also presented in terms of its equivalent refractive index change which is valuable for evaluating the voltage sensitivity of different SPR instruments. Third, we showed the ability of

Optics EXPRESS

SPR systems to detect dynamic time-resolved signals. A 100 mV signal applied over a duration of 5ms is detected with the DI-SPR system using bicell detector configuration. The signal-to-noise ratio presented in this study shows that a 10 mV signal with a temporal resolution of 5ms is achievable. Finally, a decrease in the response of the SPR system is observed when voltage with short duration is applied. This effect is attributed to slow response of the non-linear interfacial capacitance that govern the voltage sensing mechanism.

Funding

This work was supported by the Engineering and Physical Sciences Research Council [grant numbers EP/G005184/1, EP/M50810X/1]; and the University of Nottingham.

Acknowledgments

Authors acknowledge the financial support of the Engineering and Physical Sciences Research Council and the University of Nottingham, UK.